Joint particle filters prognostics for PEMFC power prediction at constant current solicitation

Marine Jouin, Rafael Gouriveau, *Member, IEEE,* Daniel Hissel, *Senior Member, IEEE,*
Marie-Cécile Péra, *Member, IEEE,* Noureddine Zerhouni *Member, IEEE*

Abstract—Proton Exchange Membrane Fuel Cells (PEMFC) are promising energy converters but still suffer from a too short life duration. Applying Prognostics and Health Management seems to be a great solution to overcome that issue. More precisely, developing prognostics to anticipate and try to avoid failures is a critical challenge. To tackle this problem, a hybrid prognostics is proposed. It aims at predicting the power aging of a PEMFC stack working at constant operating condition and constant current solicitation. The main difficulties to overcome are the lack of adapted modeling of the aging for prognostics and the occurrence of disturbances creating recovery phenomena through the aging. Consequently, this work propose a new empirical modeling for power aging that takes into account these recoveries based on different features extracted from the data. These models are used in a joint particle filters framework directly initialized by an automatic parameter estimate process. When sufficient data is available, the prognostics can give very accurate behavior predictions compared to experimentation. Remaining useful life estimates can be given with an error smaller than 5% for a horizon of 500 hours on a life duration of 1750 hours which is clearly long enough for decision making.

Index Terms—Prognostics, Particle Filter, Proton Exchange Membrane Fuel Cell (PEMFC), Aging, Remaining useful life.

ACRONYMS

ECSA	Electrochemical Surface Area
EoL	End of life
GDL	Gas Diffusion Layer
i.i.d. (noise)	Independent Identically Distributed
MAPE	Mean Absolute percent error
pdf	probability density function
PEMFC	Proton Exchange Membrane Fuel Cell
PF	Particle Filter
PHM	Prognostics and Health Management
RMSE	Root Mean Square Error
RUL	Remaining Useful Life
UKF	Unscented Kalman Filter

M. Jouin, R. Gouriveau, D. Hissel, MC. Péra and N. Zerhouni are with FEMTO-ST Institute, UMR CNRS 6174 - UFC / ENSMM / UTBM, and FC-LAB Research, FR CNRS 3539, 24 rue Alain Savary, Besançon, 25000 France. e-mails: firstname.lastname@femto-st.fr

NOTATIONS

P	stack power
a, b and c	coefficients of the power model
a_1 to a_4	coefficients in a model
b_1 to b_3	coefficients in b model
Rec	power recovery
r_1 to r_4	coefficients in Rec model
t	time index
k	time index in recursive equations
x_k	state of the system at time k
z_k	measurement at time k
$param_k$	parameter at time k
σ	noise standard deviation
i	particle index
$L()$	likelihood function

I. INTRODUCTION

A power source failure is very often dramatic as all the systems relying on it become inoperative. Anticipating such a failure thanks to Prognostics and Health Management (PHM), and more particularly to its prognostics part, can be of great concern. Especially when the considered power source is a fuel cell and that the technology considered still suffers from a too short life duration.

Fuel cells, and more precisely among all the existing technologies Proton Exchange Membrane Fuel Cells (PEMFC), are considered as promising electrical energy sources as they convert chemical energy coming from hydrogen and air into electricity, water and heat. Moreover they offer a great range of applications from transportation to micro-CHP (Combined Heat and Power generation) for building or power supply for portable devices [1]. Current PEMFC technology hardly meets the requirements for a large scale deployment: 2000 hours to 3000 hours of functioning can be achieved when 5000 hours are required for transportation applications and 100 000 hours for stationary ones.

In [2], the PHM solution is proposed to overcome the life duration issue of PEMFC. Various challenges are highlighted on all the layers of PHM, but the prognostics one is particularly empty. Indeed, although prognostics is a key process in PHM [3], [4], it just starts developing for PEMFCs. Prognostics approaches are classified in three categories: model-based, data-driven and hybrid [3]. Among these approaches, two are present in prognostics of PEMFC applications. Four different types of works can be found in the literature: two data-driven approaches using echo-state networks [5] or adaptive neuro fuzzy inference systems [6] and two hybrid prognostic

approaches with Unscented Kalman Filter (UKF) in [7] and with Particle Filter (PF) in [8]. In [7], the authors propose a prognostic model focusing on the degradation of the electrochemical surface area (ECSA) of a 1-cell PEMFC. The UKF-based framework is used to predict the decreasing of the ECSA and the Remaining Useful Life (RUL) of the cell. The results are very interesting when analyzed with the α-metric defined in [9], even if the RUL estimates are all late predictions. However, this work suffers from some drawbacks. First, it is performed on a single cell with a very short period of functioning (≈ 300 hours). By looking at the lifetime targets listed earlier, the prediction horizon remains very short and in real case applications the PEMFC is never composed of a single cell. Moreover, although tracking the ECSA evolution is a good idea as the output power of the PEMFC is closely linked to its size, this surface is hard to measure without disturbing the operation of the PEMFC. Additionnaly, this kind of *in-situ* measurements tends to aggravate the aging of the PEMFC. So this prognostics could be hardly used for real PEMFC applications.

On their side, the authors in [8] use PF to predict the voltage aging of a 5-cell PEMFC stack responding to a constant current solicitation. Three empirical models are tested to set a basis for future prognostics works. The RUL predictions are promising and allowed to validate the choice of PF as a prognostic tool for such application. Nevertheless, the use of very simple models does not allow taking into account disturbances encountered during the aging. This work is pursued in [10] in which a starting point for a solution to that limit is proposed. New models are introduced. The prognostics results start to be better, but the filters have to be initialized manually when the data or the horizon of prediction change. So although it gives interesting results, the models proposed are still incomplete and an automatic prognostics initialization has to be proposed. This paper pursues the work published in [10]. The objective here is to set a prognostics able to take into account disturbances introduced by planned characterization while estimating with a minimum error the behavior of the PEMFC. The main contributions rely on a literature review of PEMFC aging, precise models for power degradation with time varying parameters, the introduction of an automatic parameter estimate process to initialize particles filter for prognostics.

To support this, the paper is organized as follows. The first section is dedicated to PEMFC detailed presentation: the functioning principle is explained as well as the different components of the system. This allows introducing the ongoing issue of degradation understanding and modeling related to that particular system. Section **III** presents the modeling methodology adopted. The choice of using empirical models for prognostics is justified and the different steps for building an adapted set of models are explained. This set of models implies the computing of a parameter estimate process but also models' transformations to recursive forms. On this basis the association of different particle filters to perform prognostics is presented. This is the purpose of Section **IV**. It is directly followed by the application of the whole proposition in Section **V**. A comparison with our previous work [10] is made to highlight the improvement of the prognostics estimates. The results are discussed to show the strengths as well as the weaknesses that should be corrected. Finally, some concluding remarks are given.

II. BACKGROUNDS: AGING OF PEMFC

Before presenting the new framework for prognostics of PEMFC, all the key information needed to understand what will follow regarding PEMFC stacks and their aging is presented in the section.

A. System overview

A PEMFC stack is a power device that converts chemical energy into electricity, water and heat (Figure 1). To do so, it uses the oxidation of hydrogen at a first electrode, the anode, to obtain electrons that flow into an external electrical circuit and protons that go through a proton exchange membrane. These protons and electrons meet again at the second electrode, the cathode, to reduce the oxygen [11]. The electrochemical reactions involved are:

$$2H_2 \rightarrow 4H^+ + 4e^- \tag{1}$$

$$O_2 + 4H^+ + 4e^- \rightarrow 2H_2O \tag{2}$$
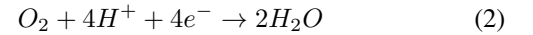
(1) occurs at the anode while (2) occurs at the cathode. The general process can be given by:

$$2H_2 + O_2 \rightarrow 2H_2O + electricity + heat \tag{3}$$

These reactions are not directly happening at the stack level but at the cell level. Indeed a stack is composed of a certain number of cells associated in series. The number of cells depends of the maximum power required from the stack. A cell is basically composed of:

- 2 bipolar plates to bring the reactant and collect electrons;
- 2 gas diffusion layers (GDL) to diffuse reactants toward the electrodes;
- 2 electrodes: anode and cathode where occur the oxidation and reduction reactions;
- 1 proton exchange membrane;
- sealing gaskets to ensure the impermeability of the cell.

As the stack is only an energy converter it cannot work on its own and different ancillaries surround it for providing reactants, controlling the operating conditions or collecting the produced electricity. For our prognostics purpose, we consider that all the ancillaries work properly with no malfunctioning and no failure. That allows us to focus only on the stack.

Operating conditions and current mission profiles are very important as far as the lifetime of a stack is concerned. Indeed, to respond in the best conditions to the current demand, operating conditions, namely temperatures, pressures, reactants flows or products evacuations, must be properly controlled. If not, it can lead to early failures preventing the stack to provide sufficient power. The value of the power is defined by the current setpoint imposed to the stack.

In this study, the current profile used in experiments remains constant and the operating conditions are kept optimal. In that way, a power drop during aging will only be the result of inner degradations of the stack. This is a major hypothesis for
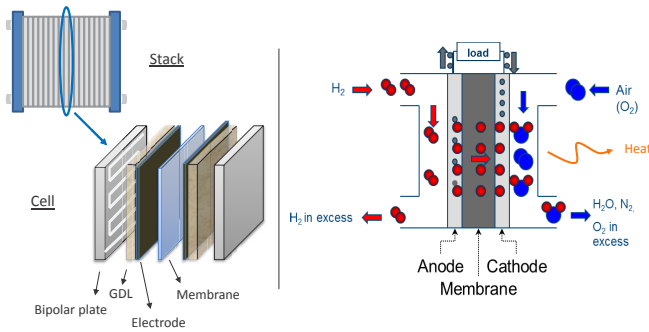
Fig. 1. Stack, cell and functioning

TABLE I
PROPOSED LECTURES FOR DEGRADATION OF COMPONENTS

Degradation type	References
Membrane aging	[19], [18], [22], [23], [24], [25], [26], [27], [28], [29], [30], [31], [32], [33], [34]
Electrodes aging	[7], [18], [20], [21], [32], [35], [36], [37], [38], [39], [40], [41], [42], [43]
GDL aging	[18], [44], [45], [46], [47], [48]
Bipolar plates aging	[20], [21], [49], [50]
Sealing gasket degradation	[21]
Aging of interfaces between components	[51], [52], [53]

all the following work. It is also important to mention that the experiments are conducted in a continuous manner. The stack was never remove from the test bench for storage, nor stopped and never experienced any current variations in an other occasion that the characterizations presented in the next paragraphs.

B. Reversibility and Irreversibility

During its lifetime, the stack looses gradually its ability to deliver its initial power. This is due to what are known in the fuel cell community as reversible and irreversible degradations. Reversible degradation refers to phenomena that lead to power losses but that can be partially or totally canceled by changing the operating conditions during a short period before returning back to nominal ones. Irreversible degradation refers to degradation as defined by the International standard [12]: "An irreversible process in one or more characteristics of an item with either time, use or an external cause". To avoid any ambiguity, the terms are redefined as follows:

- reversible degradation, that is in contradiction with the standard, is left aside in favor of "reversible" or "recoverable" phenomena,
- irreversible degradation is now simply called degradation.

The vocabulary set, some further explanations can be provided.

1) Reversible phenomena: These phenomena have been observed in a lot of works [13], [14], [15], [16] but are still not well understood. They can be caused by the interruption of the continuous testing for resting periods or for characterization with *in-situ* methods. Main reasons for reversibility of these phenomena can be water and thermal management which may change the water content and distribution in the different components in the cells [17].

2) Degradation: Degradation of a PEMFC stack is quite complex due to the different levels (stack-cell-components) and the numerous phenomena involved (chemical, electrochemical, mechanical, thermodynamics). Indeed degradations can come from:

- individual components in one cell (electrodes, membrane, etc.);
- interfaces between components of a same cell;
- interactions between two consecutive cells;
- position of a cell within the stack (in the middle or near the edge of the stack);

- gradients (temperature, water) creating heterogeneities within the stack and affecting the aging;
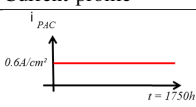- varying operating conditions accelerating some specific degradation phenomena;

All of these degradations have not been studied, and precise modeling of the ones that have been studied is very often not available. As writing a deep literature review of PEMFC degradation phenomena is not the point here, the reader may refers to [18], [19], [20], [21] for global reviews and to the references given in Table I for component-specific explanations. An important fact regarding degradation is that all the consequent dramatic failures that can prevent the stacks from providing an expected power have time constants in hours. As regards the failure definition, again it refers to the International standard [12]: "termination of the ability of an item to perform a required function". As examples, failures in a PEMFC can be the impossibility for the stack to deliver a minimum power or the impossibility of the membrane to perform its hydrogen-oxygen separator by letting the hydrogen crossing to the cathode side. Having time constants in hours is interesting for prognostics as it means that one data point per hour can be enough to use prognostic algorithms.

C. Existing aging models at the stack level

A complete aging model of a PEMFC stack should be able to take into account all previously listed: the aging of all the components within the stack, the interactions of the aging phenomena one with each others and the way they impact the efficiency of the stack, etc. Such a modeling is proposed in [54], but all the parts of the model are not explicitly given and reaching nano-scales does not seem appropriate for prognostics.

Other models focusing on voltage or power modeling seem closer to prognostics expectations. In [55], the authors propose a semi-empirical modeling of the voltage degradation at low pressures to explain and model the data observed from a PEMFC stack used in a bus. The main idea is to model the different losses that can be observed on polarization curves (i.e. curves representing the voltage in function of the current) in which the model is not time dependent in its classic form and to introduce a time dependency. The same idea is also used in [56] where a hundred stacks aged in small demonstration vehicles are modeled. But in both cases, most of the parameters of the models are empirical, so closely linked to

TABLE II
CHARACTERISTICS OF THE DATASETS

Name	Current profile	Duration	Nb charact.
D1	i_{PAC} $0.6A/cm^2$ $t = 1750h$	1750 hours	12

their data. Moreover, in the applications considered, the stacks functioned with dynamic load profiles which is not our study case.

For prognostics, modeling of the power seems the most appropriate. Indeed, the standards for PEMFC stacks end of life (EoL) are all expressed in terms of power, as in [57] where the standard EoL is set at 10% of power loss during the lifetime.

The context set, the modeling choice made for prognostics can be now explained in details.

III. MODELING OF PEMFC POWER DEGRADATION

A. Physic-based vs empirical models

To use a particle-filtering-based prognostics, an aging model of the stack is needed. Two main criteria to define this model are its complexity and the possibility to access and measure its parameters on the stack. As described before, modeling all the aging process occurring within the stack, also the reversible phenomena that cannot be ignored, can lead to very complex models. In this case leaving aside physic-based modeling and using empirical models based on parameters monitored during the experiments offers a great alternative. Moreover, as we are working with constant operating conditions and constant current demand, the influence of parameters such as temperature, reactant pressures or current has not to appear explicitly in the model. The only mandatory parameter in this application is time.

B. Data

As this can be helpful to have visual examples to illustrate the modeling process, the data used for the experiments are described. Only one dataset is available, it comes from a commercial 5-cell PEMFC stack with an active area of $100cm^2$. The measurements performed on this stack are made thanks to the test bench and procedures described in [58]. The experiment, realized on another FCLAB project, matches perfectly our hypotheses with a constant current profile and constant operating conditions and can be used for this prognostics purpose. For more clarity, the description of the dataset is given in Table II. This table provides the name that will be used in this paper for the dataset (D1), the mission profile in terms of current, the duration in hours of the experiments and also the number of characterizations performed on the stack during its lifetime.

For the experimentations, different measurements are performed:

- voltage measurements in continuous;
- current measurements in continuous (to compare with the input command);
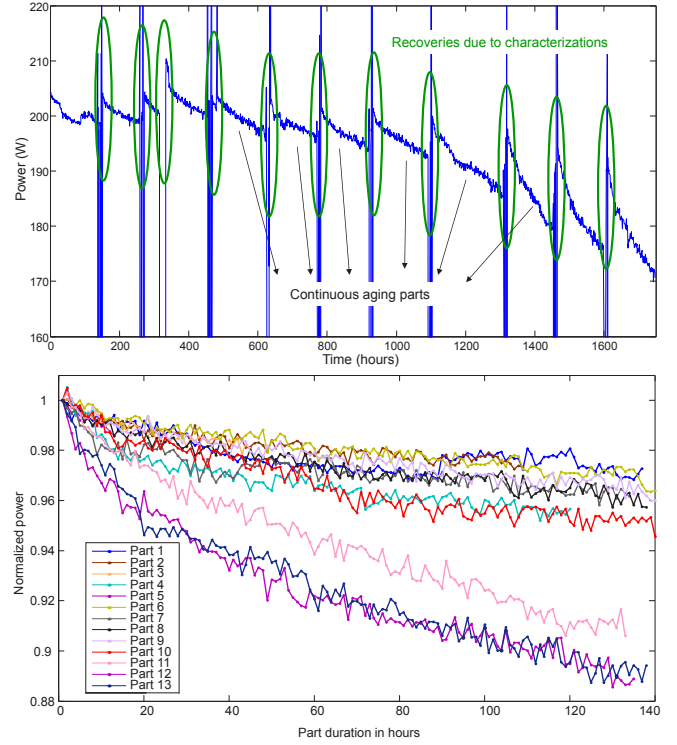

Fig. 2. Top: Dataset D1 - Bottom: Normalized voltages of the aging parts

- punctual characterizations: polarization curves + electro-chemical impedance spectroscopy.

In this study, we propose to focus only on the power delivered by the stack. Consequently, as $P = U.I$ only the voltage and current measurements are used. However, as their effects cannot be ignored, characterizations have to be mentioned. Power measurements can be seen on Figure 2.

Let's now focus on how to model the power during the aging of the stack.

C. Power global modeling

1) Formalisation: The main idea is to create a set of models that is able to describe accurately the behavior of the stack during its aging. Although it will lead to purely empirical models, it can be interesting to chose trends or descriptors that could be linked to real phenomena occurring within the fuel cell stack.

First, the data set can be divided into two types of events (see Figure 2):

1) parts of continuous aging
2) interruptions due to characterization processes

As the operating conditions and current are varying during the characterizations, these phases will not be modeled. However, assumptions will be made a little further regarding the consequences induced.

Let's focus on the different parts of continuous aging. D1 counts thirteen parts of continuous aging of different durations. Based on existing works [8], [59] and different model fittings, it appears that each part follows the equation:

$$P(t) = -a.ln(t) - b.t + c \qquad (4)$$

with t representing time but with different values of coefficients a, b and c. For comparison purpose, t is set to zero in the beginning of each segment. This empirical modeling is now justified by actual phenomena occurring within the stack.

2) Justification: It can be observed that as time evolves, the aging effects occur faster and faster leading to more serious power drop. Moreover the impact of the logarithmic part of the model seems to accentuate and last longer. It is illustrated in the bottom part of Figure 2, which shows the normalized powers of all segments to compare them visually. It is resulted from dividing the power by its initial value in each segment. This can be explained if we give a physical meaning to the different parts of the model. Due to the diffusion phenomena of gas and water and also to reversible phenomena, the stack goes through a transient phase after the operating conditions are set to their nominal values. It is represented by the logarithmic part of the model. Once that transient phase is over, the stack enters a steady power decay represented by the linear part. This distinction between the transient and steady parts is further explained in [14]. As the stack ages, its components might have some difficulties to fulfill their functions leading, for example, to slower gas diffusion through the gas diffusion layers, to presence of contaminants at the membrane and electrodes or to greater water accumulation at the cathode by loosing hydrophobic properties. Combined together, these phenomena, coming from both degradation and reversible events, may lead to longer transient phases with a greater power drop. Degradation, namely of conductivity and activity of the membrane and the electrodes, also lead to more severe power drop during the steady state, reflected by greater coefficients in the linear part of the model.

It is now obvious that our model coefficients, a and b (c left apart because not used afterward), will evolve with time. It can be interesting to figure out if they will follow particular predictable trends.

D. Parameter trend modeling

To extract trends for a and b from (4), these coefficients are determined by fitting the equation to the data on the different aging segments. The whole data set is used to that goal. Equation (4) is fitted successively to all the aging segments and the different values of a and b are determined. This is achieved by using a least squares fitting. These values, which are constant in each segment, are shown on Figure 3 by the blue dots. Both coefficients seem to follow trends that can be modeled easily with exponential functions (Figure 3, red curves). Indeed the evolution of the transient phase (coefficient a) can be easily modeled by:

$$a(t) = a_1.exp(a_2.t) + a_3.exp(a_4.t) \quad (5)$$

whereas the acceleration of the linear part is harder to model precisely:

$$b(t) = b_1.exp(b_2.t) + b_3 \quad (6)$$

However, although this last seems less obvious when the global trend is compared to the data, it might not be so far from the reality. Indeed, the authors in [60] showed that the degradation rate for constant current follows a bathtub-like curve. Here,
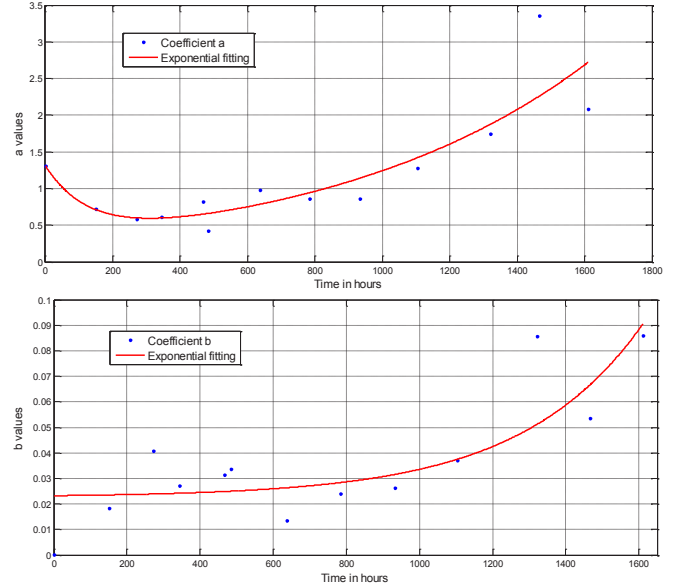

Fig. 3. Trends extracted for coefficients a and b

if we consider that the linear part of the model (4) can be assimilated to a degradation rate in a steady state and that the stack has already left its early life (manufacturers usually let the stack working around 100 hours to leave the early life stage before delivering the stack to the customers), the equation (6) can find a justification.

Now that we are able to model the different continuous aging part, we have to wonder what the initial power at the starting point of each part is .

E. Recovery modeling

After each characterization phase, the stack seems to recover some power (see Section II-B). However, it is not clearly explained. It may be linked to change in gas and liquids' repartitions within the stack when the operating conditions return to their nominal values after variations during the characterizations. It can be seen on Figure 4 that this recovery does not remain constant during the aging. In terms of difference of power between and after the characterization phase, it increases. But by looking at the values reached after all the characterizations, the maximum recovery power decreases with time. Indeed, as the stack ages, the recovery is limited by the degradation of the stack components.

For our prognostics purpose, we choose to follow the evolution of the maximum recovery power through time. As for the previous parameters, the recovery is extracted from the data and a global trend of it as aging is found. It follows an exponential form:

$$Rec(t) = r_1.exp(r_2.t) + r_3.exp(r_4.t) \quad (7)$$

This exponential trend is not a surprise, it is coherent with the fact that the main degradations impacting the power drop follow exponential trends. Among these degradations, the loss of active surface area [7] and the increase of hydrogen crossover from the anode to the cathode [20], [31] can be
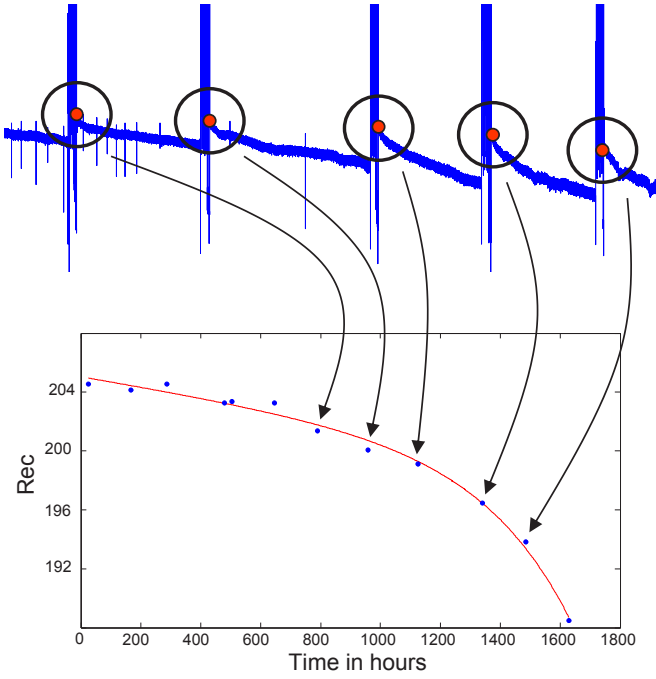
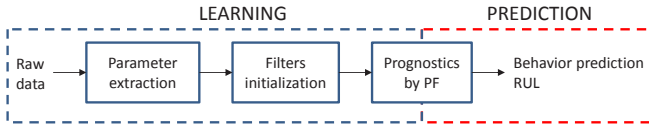Fig. 4. Trend extracted for the recovery

Fig. 5. Prognostics framework

highlighted.

In this part, we have selected different parameters and built models that will help follow the aging of the stack. To stick to the reality, all the parameters chosen can have physical interpretations. This has now to be integrated in a prognostics framework to help predicting the remaining useful life of PEMFC stacks.

IV. PROGNOSTICS OF PEMFC

To achieve power behavior prediction and RUL estimation, our prognostics framework is divided in two main part:

1) a parameter extraction part;
2) a particle filter-based prognostics.

This is illustrated by Figure 5. The main reason why parameter extraction and prognostics are computed together is that the parameter estimate part directly creates the initial distributions needed by the particle filters. When the length of the learning set varies, the parameter estimate results change giving different initializations to the prognostic part. As more data become available, the parameter estimate part gives better results and this directly impacts the prognostics predictions. Before detailing the whole framework, a short reminder on particle filters theory is given here.

A. Particle filters

Particle filters are great tools to solve nonlinear Bayesian tracking problems. Indeed, the models defined above meets completely the hypotheses of this kind of problems as they are nonlinear, non-exact (with unknown coefficients), non-stationary and they might contain non Gaussian noise.
A Bayesian tracking problem is defined by two equations [61], [62]:

- the state equation

$$x_k = f(x_{k-1}, \vartheta_k, \nu_k) \quad (8)$$

- and the observation model

$$z_k = h(x_k, \mu_k) \quad (9)$$

In the state equation, $\{x_k, k \in \mathbb{N}\}$ represents the state that has to be followed and predicted, ϑ_k parameters of the model and ν_k an independent identically distributed (i.i.d.) noise. These variables change at each step and the passage from step $k-1$ to k is made thanks to the transition function f. Regarding the observation model, $\{z_k, k \in \mathbb{N}\}$ represents the measurements, μ_k an i.i.d. noise and h the observation function. As measurements are directly available from the data, no observation model has to be built in this work.
To obtain a distribution of the possible states of x at time k, the probability density function $p(x_k|z_{1:k})$ has to be built. The starting point is given by the initial state distribution $p(x_0|z_0) \equiv p(x_0)$. It is assumed that this initial pdf is known. The optimal Bayesian solution is obtained by repeating a prediction and an update stages:

1) prediction

$$p(x_k|z_{1:k-1}) = \int p(x_k|x_{k-1})p(x_{k-1}|z_{k-1})dx_{k-1} \quad (10)$$

2) update

$$p(x_k|z_{1:k}) = \frac{p(z_k|x_k)p(x_k|z_{1:k})}{p(z_k|z_{1:k-1})} \quad (11)$$

However, this optimal solution cannot be obtained analytically in most of the cases. Here comes the particle filter to give an approximate solution.
Particle filters are from the family of Monte Carlo-based tools using the Baye's theorem as basis. The first stage consists in splitting the initial state distribution $p(x_0)$ into n samples named particles. Three steps are then repeated until the desired results is obtain (Figure 6):

1) Prediction: particles are propagated thanks to the state model from step $k-1$ to k giving a new pdf.
2) Update: the measurement z_k is used to calculate the likelihood function $p(z_k|x_k)$ and give weights to the particles. Particles representing states close the last measurement have the higher likelihood and represent the most probable states.
3) Re-sampling: particles with the lower weights are eliminated and particles with the higher weights are manifolded. This procedure allows avoiding a degeneracy of the filter, namely the increasing number of particles
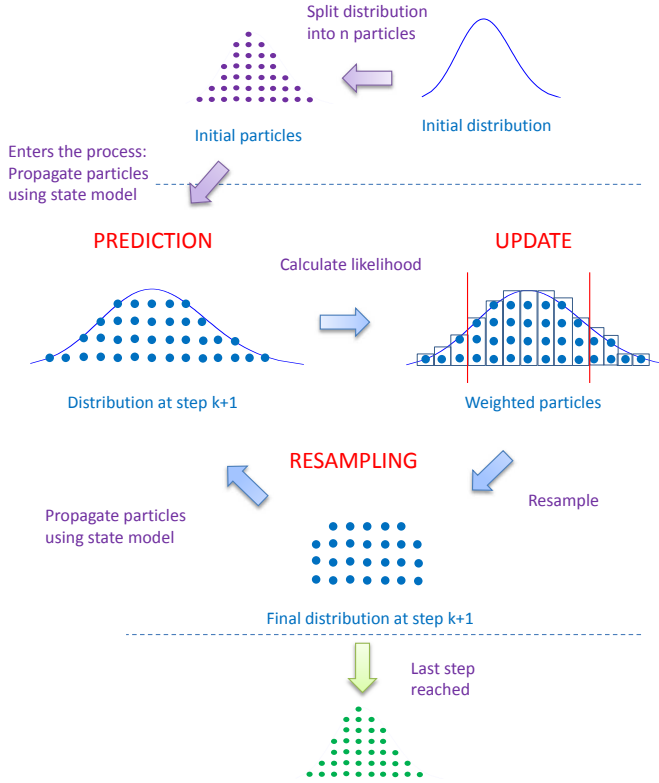
Fig. 6. Particle filter principle

with low weights that would lead to bad results in the previous stages.

This process is applied all along the learning of the prognostics. In fact, as soon as no data become available, no measurements z_k can be used to calculate the likelihood function and the prognostics enters its prediction phase. In that step, the particles are simply propagated by the state model. Once the failure threshold is reached, the final distribution of the particles give the most probable state, i.e., the state represented by the weighted average of the particles, and its uncertainty distribution, i.e., the distribution of the particles.

B. Parameter extraction

1) Parameter extraction on raw data: The raw data at the entry of the parameter extraction box is composed of the power signal and the characterization calendar. Thanks to the calendar, the different parts of continuous aging available for the learning are identified. The fitting procedure uses the data to identify the coefficients a and b from equation (4). A robust least squares algorithm is used for that purpose. The recovery values after each characterization are also identified at that stage. These values are stored in tables.

2) Model identification and filter initialization: In the previous section, we have defined four models and three of them (5) to (7) have unknown coefficients that should be identified. Thanks to the data stored in the previous step the parameters a_1 to a_4, b_1, b_2 and r_1 to r_4 are estimated. As their identification relies on values estimated on the previous step, these estimates may come with uncertainties. As our procedure

does not estimate this uncertainty, we decide to associate uncertainty ranging from $\pm 1\%$ to $\pm 5\%$ depending on the order of magnitude of the parameter. Consequently, our model identification directly gives us distributions for intializing the particle filters used just after. These distributions are uniform distributions centered on the value obtained by identification with a width given by the associated uncertainty.

This step imposes a first limitation to the prognostics framework. Indeed, as equations (5) and (7) have each one four coefficients to identify, it implies that four characterizations have already been performed in the data used for the learning. Now that the extraction of parameters is done, the information extracted is used to perform prognostics.

C. Joint particle-filtering-based prognostics

For the record, the final objective of that work is to predict the behavior of the power delivered by the stack through time and to estimate the RUL at various points in time. To achieve this goal, we have a global power model (4) and three other models dedicated to specific parameters from model (4). As all the future evolutions of these models have to be predicted, a framework with four particle filters is set. Of course, the framework could have been reduced to two by including equations (5) and (6) in the first one. But, in order to evaluate the quality of the different models, keeping them separate is more interesting for further investigation.

To integrate them in the particle filters as state equations, all the equations have to be written in a recursive manner. However, one important assumption is made regarding the global power model: coefficients a and b remain constant on the full length of a continuous aging part. This assumption is made to remain consistent with the way these parameters were extracted in the first place. The continuous aging parts are numbered and this is represented by the index i in the next equation. Consequently, although the parameters a and b are estimated continuously, only the first value estimated at the beginning of the aging part i is stored as a_i and b_i. Then when a characterization happens and a new aging part starts, the last value of a and b obtained at time (k + length of segment i) is used to define a_{i+1} and b_{i+1}. So, the characteristics of the different filters are as follows:

- Filter 1: Global power
  - State equation:

$$P_k = a_i.log(k - 1/k) - b_i + P_{k-1} \quad (12)$$

  - Measurements: power obtained from voltage and current measurements
- Filter 2: Coefficient of the logarithmic part a
  - State equation:

$$a_k = a_1.exp(a_2.k).(1 - exp(-a_2))$$
$$+ a_3.exp(a_4.k).(1 - exp(-a_4)) + a_{k-1} \quad (13)$$

  - Measurements: values of a extracted during the parameter extraction
- Filter 3: Coefficient of the linear part b

– State equation:

$$b_k = b_1.exp(b_2.k).(1 - exp(-b_2)) + b_{k-1} \quad (14)$$

– Measurements: values of b extracted during the parameter extraction
- Filter 4: Power recovery
  – State equation:

$$Rec_k = r_1.exp(r_2.k).(1 - exp(-r_2))$$
$$+ r_3.exp(r_4.k).(1 - exp(-r_4)) + Rec_{k-1} \quad (15)$$

– Measurements: recovery extracted during the parameter extraction

It can be noticed that no noise has been introduced in the different state equations. As general trends and not precise models are expected, we consider that this noise can be ignored for prognostics. As far as the measurement noises are concerned, as the raw data are used, the noise is already included in them. So for each filter, the z_k used are the noisy measurement. However, the noise contained in z_k should be taken into account when comparing the filter estimation to the actual data. As the characteristics of the noise are unknown in that application, it is assumed that it is a Gaussian noise with an unknown standard deviation σ. It allows to use the method proposed in [63]. It states that the standard deviation of the measurement noise can be considered as a variable to be estimated and that it becomes part of the state vector. Consequently, this standard deviation is estimated and propagated thanks to the particles. It then intervenes when the likelihood of each particle is calculated which becomes a function of the state, the model parameters and the noise standard deviation estimates: $L(z_k|x_k^i, param_k^i, \sigma_k^i)$.

The four filters are working in parallel, synchronized on the same time step. During the period of continuous aging, they are all predicting their attributed state model with no interaction with each other. When the date of a characterization is met, the particles distributions for parameters a and b in Filter 1 are updated thanks to the last distributions predicted by Filter 2 and Filter 3. Moreover, the last distribution of the recovery Rec_k is used to replace the state particles of P_k. This process is represented on Figure 7 for more clarity.

D. Uncertainty propagation

The uncertainty coming all along the prognostic process is one of the major issues of prognostics applications. This uncertainty may come from the data, the parameter estimate and the prognostic part. Consequently, all the framework was built to take into account the uncertainty and to propagate it from one step to another.

Regarding the extraction part, the treatment of uncertainty has already been explained: distributions centered on the parameters identified are drawn. For the prognostics part, the uncertainty propagation is ensured by Filter 4 before the last characterization and after by Filter 1. Indeed, as particle filters are working with particle distributions, they naturally give the uncertainty coming with the prediction (see Section IV-A). As the power given by Filter 1 is regularly updated by external
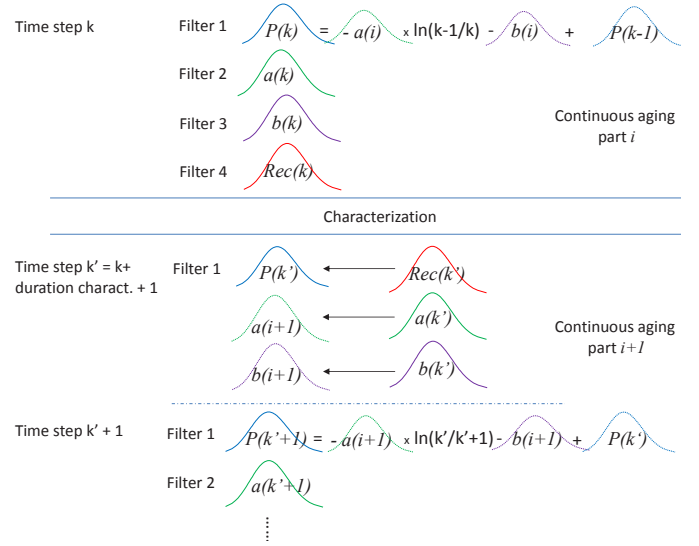

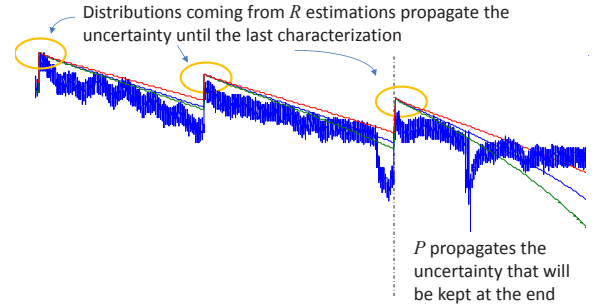Fig. 7. Filters interactions between and just after characterizations

Fig. 8. Models role in uncertainty propagation

parameters, the uncertainty coming with power behavior predictions changes after each characterization. When the power is concerned, only the recovery prediction given by Filter 4 propagates the same uncertainty from the beginning to the last characterization. After this last one, the last distribution given by Rec is used by Filter 1 to predict the power until the failure threshold (Figure 8).

By proceeding that way, the RUL distribution, which is the final goal of our prognostics framework, takes into account all the possible sources of uncertainty of the framework.

To demonstrate the ability of this framework to give good predictions, series of tests are performed on the dataset presented earlier.

V. EXPERIMENTS AND DISCUSSION

A. Experiment settings

The main parameters to define for these experiments are the EoL threshold and the length of the learning. Regarding the threshold, by referring to what is explained earlier, it should be set at 10% of the initial power value. Nevertheless, if this threshold is respected, only a small part of the data would be used: power would be around 184 W corresponding to less than 1300 hours. To benefit from all the data available, the EoL threshold is chosen to be located at 16.3% of the initial power.
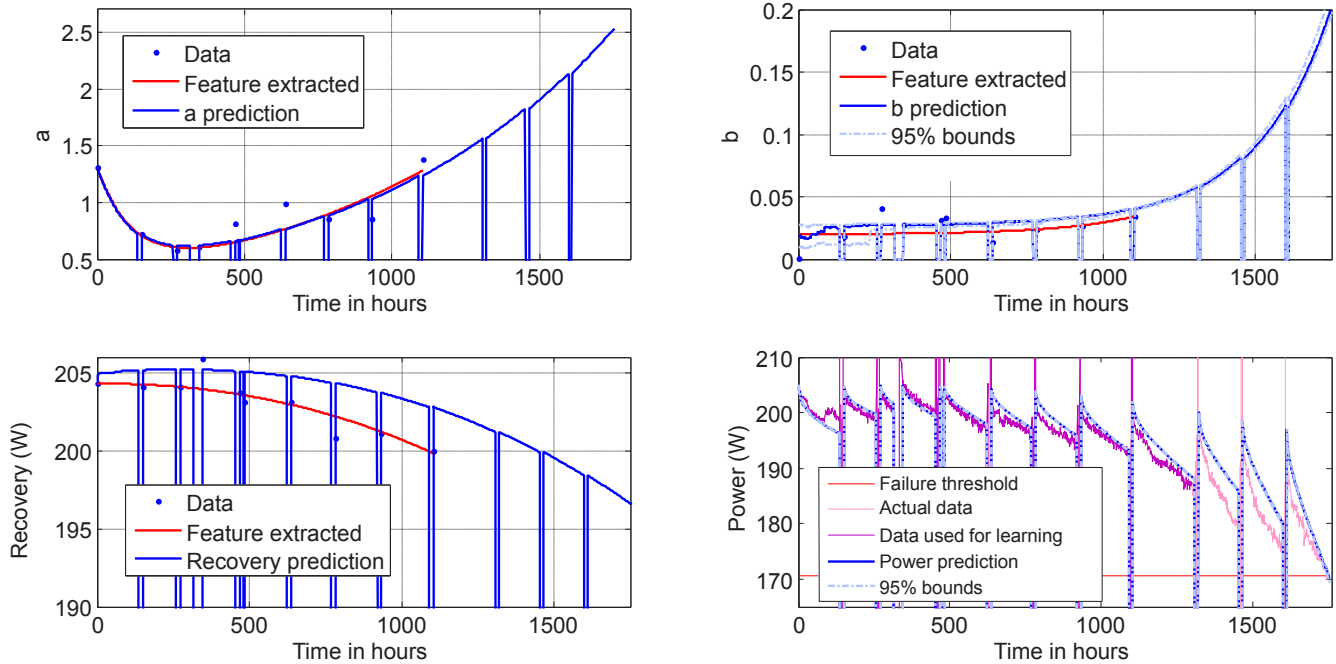
Fig. 9. Example of results for a learning of 1300 hours

This value is calculated thanks to the difference between the value of the power at t=0 and the value at the end of the experiments.

Then, the learning length has to be defined. In order to estimate the largest prediction horizon that can be reached with a reasonable prediction error, different length of learning are tested from 500 hours to 1700 hours with a step of 100 hours. The minimum value of 500 hours cannot be reduced as at least four points are needed to identify coefficients in equations (5) and (7).

It is also important to mention that the four particle filters are SIR (Sampling Importance Resampling) type [62]. The filters are programmed in Matlab language and inspired from [63]. To avoid any degeneracy problem during the testing, they are all working with 10 000 particles. This can take a long computing time for obtaining results, but this duration is not yet a performance criterion in this work.

Before showing the results, it should be mentioned that in Figures 9, 11 and 15, vertical lines appear at the time of characterizations as already observed in Figure 2. As the current varies during the characterization breaking the hypothesis of constant current solicitation for prognostics, no prediction is made during that period. For convenience of use, the state vector is filled with zeros at the dates of these events creating the vertical lines.

B. Power aging predictions

1) General comments: For each learning the prognostics returns the curves shown on Figure 9. The left upper part represents the prediction of the coefficient a by Filter 2, the right upper part shows b predicted by Filter 3, the left lower part shows the recovery from Filter 4 and finally the last part presents the power predictions by Filter 1. For illustration

purpose, the confidence interval given by the filters appears on the power and b graphs. A zoom of the confidence interval coming with power aging can be found on Figure 10.

The results obtained for power aging predictions can be divided in two parts according to the duration of the learning: bad predictions with a learning between 500 and 1100 hours and good predictions for 1200 hours and more. Indeed, for small learnings, the models seems to fail catching the behavior of the stack (Figure 11). It indicates that one or more parameters of the models cannot be predicted accurately.

2) Parameter estimate vs learning duration: The results given by the prognostics are strongly determined by the parameter estimate part. Indeed, when very few points are available identifying parameters a, b and Rec trends by fitting their models can lead to false approximations. As more data become available, the trends start to draw closer to the reality. This can clearly be seen on Figure 12.

The recovery Rec seems to be the major limitation when less than six points are available, corresponding to a learning of
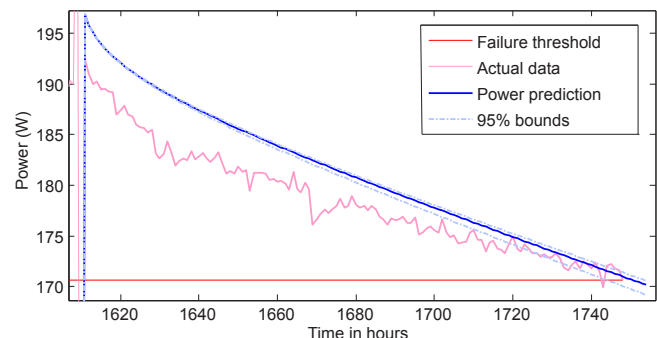

Fig. 10. Zoom on the confidence interval for power prediction at 1300 hours

TABLE III
RMSE AND MAPE DURING PREDICTIONS

Learning	500	600	700	800	900	1000	1100
RMSE (hours)	15,7	40,9	11,8	10,3	8,9	9,4	4,8
MAPE (%)	1,57	5,06	4,77	4,04	3,92	4,21	1,97

1200	1300	1400	1500	1600	1700
3,2	4,9	3,3	3,9	1,1	0,7
1,29	2,49	1,33	1,92	0,45	0,33

700 hours. The exponential part of the model is not well identified leading to a sudden drop in Rec trend. This partly explains that prognostics for learnings of 500, 600 and 700 hours stop very early.

For 700 hours, another part of the explanation concerns the coefficient a driving the logarithmic part of the model. For short learnings, this coefficient is not well estimated. Some of the extreme data points are gathered between 500 and 700 hours preventing the parameter estimate from approximating the good trend. However, after 1000 hours the feature extracted starts to converge toward the real trend.

Regarding the coefficient b which drives the linear part of the model, the parameters extracted are more dispersed and most of the time overestimates the trend. The impact of this dispersion is noteworthy on the results for short training, particularly for 900 and 1000 hours where a negative sign appears. However, it seems that the overestimation of this coefficient is more or less counterbalanced in the power aging prediction by the error on a approximation.

3) Evaluation of the error: To further evaluate the predictions, it can be interesting to take a closer look a the RMSE and the MAPE observed during learning and prediction for the different learning duration (Figure 13 and Table III).

For the learning the MAPE is bounded between 0.4% and 0.9% with a mean of 0.574%. As regards predictions, the MAPE seems to decrease exponentially with the increasing of the learning duration. This is more visible by using the RMSE values available in Table III. The maximum MAPE value is 5.06% obtained for a learning of 600 hours to reach its minimum of 0.33% for 1700 hours. The decreasing is logical, as when more data become available and the EoL is closer, the predictions become more accurate. These values also reflect what happens on Figure 11 and the ability of the models to predict the behavior as discussed above.
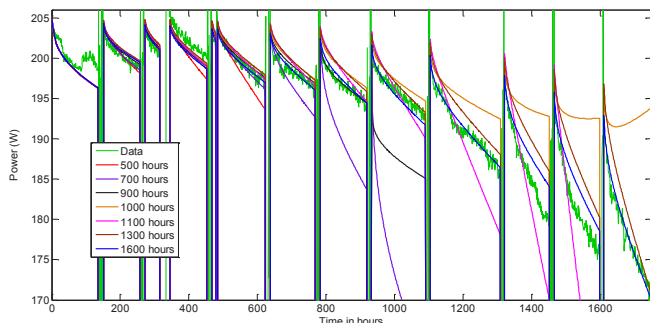

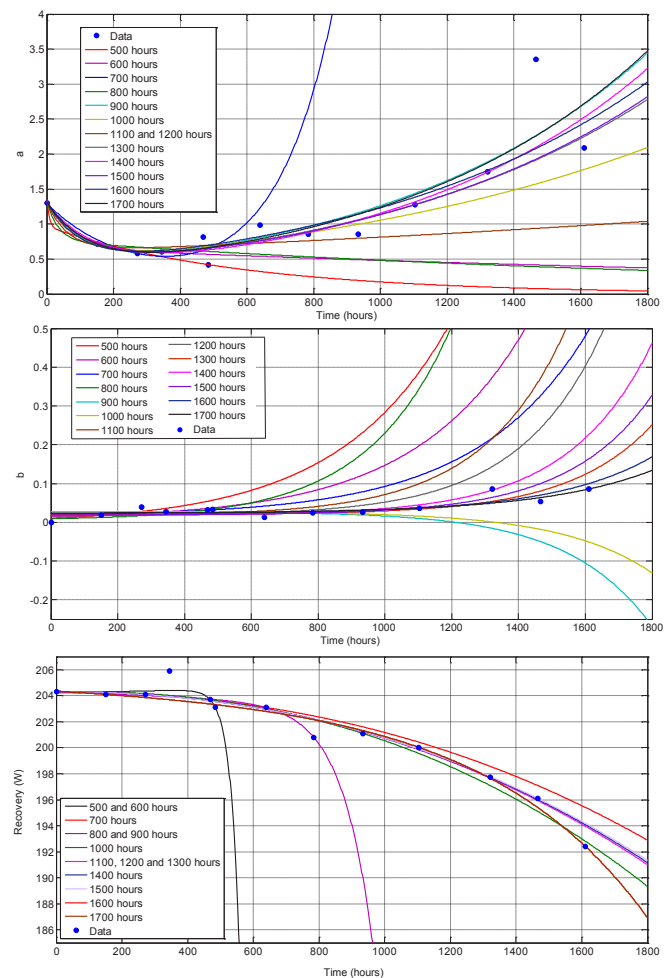Fig. 11.   Predictions for different learnings

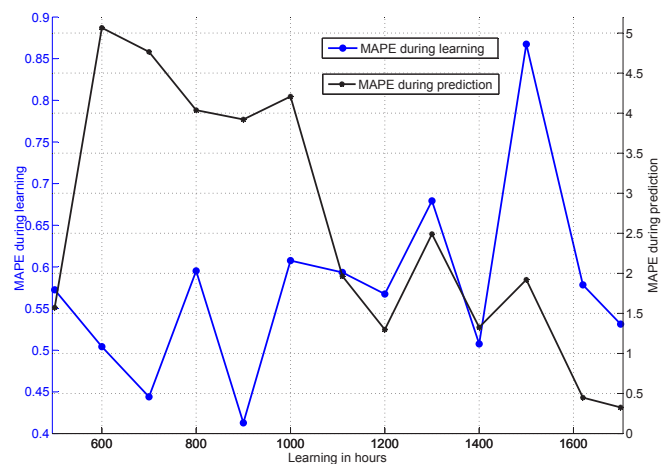Fig. 12.   Parameter estimates with different learnings

Fig. 13.   MAPE during the learning and prediction stages function of the length of the learning

C. RUL estimates

Calculating and representing the remaining useful life evolution through time can give us an idea of the prognostics horizon that can be expected from the framework. Figure 14 shows the RUL estimates with the lower and upper bounds of
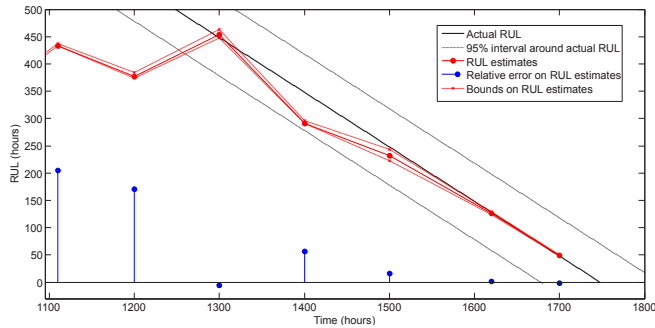
Fig. 14. RUL evolution through time

Learning	Lower bound	Upper bound	Dispersion
1100	RUL - 0.2	RUL + 3.9	4.1
1200	RUL - 3,5	RUL + 7.4	10.9
1300	RUL - 6.6	RUL + 9.6	16.2
1400	RUL - 0	RUL + 4.7	4.7
1500	RUL - 9.5	RUL + 11.5	21
1600	RUL - 2.4	RUL + 3.7	6.1
1700	RUL - 0.4	RUL + 1.7	2.1
Mean	RUL - 3.2	RUL + 6.1	9.3

TABLE IV
DETERMINATION OF THE MAXIMUM PREDICTION HORIZON

Learning	Horizon	RUL	Error (Act. - Estim.)	%
1210	538	383	155	40.5 %
1220	528	494	34	6.9 %
1230	518	497	21	4.2 %
1240	508	495	13	2.6 %
1250	498	514	-16	3.1 %
1260	488	533	-45	8.4 %
1270	478	519	-41	7.9 %
1280	468	476	-8	1.7 %
1290	458	454	4	0.9 %

their distribution (red lines) and also the relative error between actual RUL and estimates (blue lines). Only the results for a learning equal and greater than 1100 hours are shown on this figure, as all the previous estimates exhibit errors greater than 600 hours. The reasons for that have already been discussed earlier.

RUL estimates are very promising. Indeed, for a learning greater than 1300 hours, the maximum relative error is 57 hours for 1400 hours. It means that for a prediction horizon of 450 hours, the RUL can be given with an error smaller than 5%. To define more precisely what could be the larger horizon with a maximum error of 5%, new tests are launched. The step between two prediction is reduced from 100 hours to 10 hours. The results are summarized in Table IV. Although the error is twice superior to 5% after that date, the maximum horizon seems to be located around 518 hours for a learning. Assuming that the stack is working continuously, it gives 21 days to react and to take the right mitigation actions which is fairly correct.

It can be seen thanks to RUL bounds on Figure 14 and Table V that RUL distributions are very small. Indeed, the larger RUL distribution is obtained for a learning of 1500 hours and it is 21 hours long but the mean value is 9.3 hours. This demonstrates a very small uncertainty coming with RUL estimates. In a real case application, it means that the date when the stack is going to reach its EoL could be known to the precision of a single day. Considering that almost all the prediction are early predictions, the prognostics will be very interesting for deciding mitigation strategies or system maintenance.

D. Comparison with previous work

As a comparison between models that take into account disturbances (in [10]) and those that don't (in [8]), was already done in [10], showing the improvement in estimating the state and reducing the prognostics uncertainty, this comparison only focuses on comparing the results presented here and those presented in [10]. The EoL threshold was exactly the same as in this paper.

As stated in the introduction, the main differences rely in the modeling and in the automatic initialization of the filters. In [10], no modeling for a existed and the only variations of the parameter was due to the estimation of the particle filter in charge of power prediction. Without the model, the linear part was dominating leading to poor behavior estimations on the parts where the logarithmic effect was accentuating. The RUL estimates seemed to be globally better mainly thanks to 2 factors:

1) the behavior prediction luckily meets the EoL threshold at the right place, if another threshold was defined the RUL estimates would not be so good;
2) the particle filters were manually initialized, different tries were required to define the initial distributions that would lead to acceptable results: in practical applications such a practice would not be usable.

So, the RUL estimates are left apart and only the behavior prediction is considered. Figure 15 shows both the old and new models behavior estimations when using all the data available for training. The new model catches better the behavior of the power during the aging of the stack. The adding of the logarithmic part modeling improves clearly the results. Moreover, it shows that the automatic initialization of the filters can lead to results as good as for manual initialization, with the exception of the learning duration limitation.

E. Discussion

The analysis of the results shows some good points as well as some limitations to the prognostics developed here. First, the occurrence of the characterizations is defined by a calendar. This calendar is known to perform prognostics. The framework should also be able to deal with unplanned characterization. Then, modeling independently the different phenomena related to the occurrence of disturbances seems to be a good solution. Indeed, it allows modeling precisely the aging of the different parameters with time. The empirical expressions defined for each of them are simple but sufficient to obtain behavior
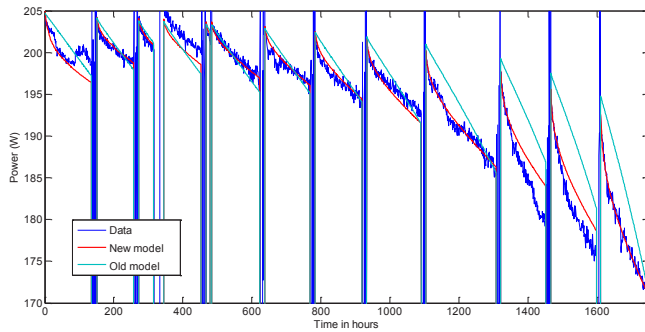
Fig. 15. Comparison between the old model from [10] and the new model

predictions with a small MAPE. But using different models with unknown coefficient also creates one major limitation of that work: the amount of data needed to have good trends from the parameter estimate based on the least squares method covers more than 1100 hours which is around 60% of the stack lifetime in this case study. Using a different parameter extraction method could be a solution to that problem. Trying to find a deeper link with physics to have fix values of some coefficients might be another one.

VI. CONCLUSION

This work presents a new modeling for prognostics of PEMFC under constant current solicitation but facing events creating disturbance in the natural aging behavior. A global model for power aging is set including time-variant parameters. These parameters can be modeled independently as they show specific trend as the stack degrades. Moreover, they allow highlighting different physical phenomena as transient effects, steady state aging and recoveries.

These models are parts of a global prognostics framework composed by a parameter extraction part and a particle filtering part. The automatic parameter estimate based on least square fitting allows identifying the unknown coefficients of all the models and thereby initializing four particle filters. These lasts interact together to allow predicting the power aging of the stack and estimating the remaining useful life.

The whole proposition is quite convincing as it can predict the RUL with less than 5% of error with a horizon of more than 500 hours. However, a major limitation relies in the length of the data needed for the learning as more than 1100 hours are needed, covering more than the half of the stack life. Consequently, the parameter estimate part should be improved to use less data while the prognostics keeps offering good results.

To ensure that this prognostics is sufficiently generic, new experiments are conducted to provide new aging data coming from different fuel cell stacks. Once this method is definitely validated, the next step of this work will be to include the current in the modeling and so being able to manage variable current profiles. This will lead to prognostics closer to real automotive or stationary applications.

REFERENCES

[1] O. Z. Sharaf and M. F. Orhan, "An overview of fuel cell technology: Fundamentals and applications," *Renewable and Sustainable Energy Reviews*, vol. 32, pp. 810 – 853, 2014.

[2] M. Jouin, R. Gouriveau, D. Hissel, M.-C. Péra, and N. Zerhouni, "Prognostics and health management of PEMFC state of the art and remaining challenges," *International Journal of Hydrogen Energy*, vol. 38, no. 35, pp. 15 307 – 15 317, 2013.

[3] R. Gouriveau and N. Zerhouni, "Connexionist-systems-based long term prediction approaches for prognostics," *Reliability, IEEE Transactions on*, vol. 61, no. 4, pp. 909–920, Dec 2012.

[4] E. Ramasso and R. Gouriveau, "Remaining useful life estimation by classification of predictions based on a neuro-fuzzy system and theory of belief functions," *Reliability, IEEE Transactions on*, vol. PP, no. 99, pp. 1–1, 2014.

[5] S. Morando, S. Jemei, R. Gouriveau, N. Zerhouni, and D. Hissel, "Fuel cells prognostics using echo state network," in *Industrial Electronics Society, IECON 2013 - 39th Annual Conference of the IEEE*, 2013, pp. 1632–1637.

[6] R. Silva, R. Gouriveau, S. Jemei, D. Hissel, L. Boulon, K. Agbossou, and N. Y. Steiner, "Proton exchange membrane fuel cell degradation prediction based on adaptive neuro fuzzy inference systems," *International Journal of Hydrogen Energy*, vol. to appear, 2014.

[7] X. Zhang and P. Pisu, "An unscented kalman filter based approach for the health-monitoring and prognostics of a polymer electrolyte membrane fuel cell," in *Proceedings of the annual conference of the prognostics and health management society*, 2012.

[8] M. Jouin, R. Gouriveau, D. Hissel, M.-C. Péra, and N. Zerhouni, "Prognostics of PEM fuel cell in a particle filtering framework," *International Journal of Hydrogen Energy*, vol. 39, no. 1, pp. 481 – 494, 2014.

[9] A. Saxena, J. Celaya, B. Saha, S. Saha, and K. Goebel, "On applying the prognostic performance metrics," in *Proceedings of the annual conference of the prognostics and health management society*, 2009.

[10] M. Jouin, R. Gouriveau, D. Hissel, M.-C. Péra, and N. Zerhouni, "Prognostics of proton exchange membrane fuel cell stack in a particle filtering framework including characterization disturbances and voltage recovery," in *Proceedings of the 2014 IEEE International Conference on Prognostics and Health Management - To appear*, 2014.

[11] J. Larminie, A. Dicks, and M. S. McDonald, *Fuel cell systems explained*. Wiley Chichester, 2003, vol. 2, no. 1.

[12] B. S. I. Staff and B. S. Institution, *European Standard EN 13306*. British Standards Institution, 2001.

[13] S. Cleghorn, D. Mayfield, D. Moore, J. Moore, G. Rusch, T. Sherman, N. Sisofo, and U. Beuscher, "A polymer electrolyte fuel cell life test: 3 years of continuous operation," *Journal of Power Sources*, vol. 158, no. 1, pp. 446 – 454, 2006.

[14] S. Kundu, M. Fowler, L. C. Simon, and R. Abouatallah, "Reversible and irreversible degradation in fuel cells during open circuit voltage durability testing," *Journal of Power Sources*, vol. 182, no. 1, pp. 254 – 258, 2008.

[15] J. Wu, X.-Z. Yuan, J. J. Martin, H. Wang, D. Yang, J. Qiao, and J. Ma, "Proton exchange membrane fuel cell degradation under close to open-circuit conditions: Part i: In situ diagnosis," *Journal of Power Sources*, vol. 195, no. 4, pp. 1171 – 1176, 2010.

[16] M. Prasanna, E. Cho, T.-H. Lim, and I.-H. Oh, "Effects of MEA fabrication method on durability of polymer electrolyte membrane fuel cells," *Electrochimica Acta*, vol. 53, no. 16, pp. 5434 – 5441, 2008.

[17] F. Wang, D. Yang, B. Li, H. Zhang, C. Hao, F. Chang, and J. Ma, "Investigation of the recoverable degradation of PEM fuel cell operated under drive cycle and different humidities," *International Journal of Hydrogen Energy*, no. 0, pp. –, 2014.

[18] R. Borup, J. Meyers, B. Pivovar, Y. S. Kim, R. Mukundan, D. Garland, N.and Myers, F. Wilson, M.and Garzon, D. Wood *et al.*, "Scientific aspects of polymer electrolyte fuel cell durability and degradation," *Chemical reviews*, vol. 107, no. 10, pp. 3904–3951, 2007.

[19] F. De Bruijn, V. Dam, and G. Janssen, "Review: durability and degradation issues of pem fuel cell components," *Fuel Cells*, vol. 8, no. 1, pp. 3–22, 2008.

[20] W. Schmittinger and A. Vahidi, "A review of the main parameters influencing long-term performance and durability of PEM fuel cells," *Journal of Power Sources*, vol. 180, no. 1, pp. 1 – 14, 2008.

[21] J. Wu, X. Z. Yuan, J. J. Martin, H. Wang, J. Zhang, J. Shen, S. Wu, and W. Merida, "A review of PEM fuel cell durability: Degradation mechanisms and mitigation strategies," *Journal of Power Sources*, vol. 184, no. 1, pp. 104 – 119, 2008.

[22] A. Collier, H. Wang, X. Z. Yuan, J. Zhang, and D. P. Wilkinson, "Degradation of polymer electrolyte membranes," *International Journal of Hydrogen Energy*, vol. 31, no. 13, pp. 1838 – 1854, 2006.

[23] C. S. Gittleman, F. D. Coms, and Y.-H. Lai, "Chapter 2 - membrane durability: Physical and chemical degradation," in *Polymer Electrolyte Fuel Cell Degradation*, M. M. Mench, E. C. Kumbur, and T. N. Veziroglu, Eds. Academic Press, 2012, pp. 15 – 88.

[24] A. Kusoglu, A. M. Karlsson, M. H. Santare, S. Cleghorn, and W. B. Johnson, "Mechanical response of fuel cell membranes subjected to a hygro-thermal cycle," *Journal of Power Sources*, vol. 161, no. 2, pp. 987 – 996, 2006.

[25] Y.-H. Lai, C. K. Mittelsteadt, C. S. Gittleman, and D. A. Dillard, "Viscoelastic stress model and mechanical characterization of perfluo-rosulfonic acid PFSA polymer electrolyte membranes." ASME, 2005.

[26] R. Solasi, Y. Zou, X. Huang, K. Reifsnider, and D. Condit, "On mechanical behavior and in-plane modeling of constrained PEM fuel cell membranes subjected to hydration and temperature cycles," *Journal of Power Sources*, vol. 167, no. 2, pp. 366 – 377, 2007.

[27] R. Solasi, Y. Zou, X. Huang, and K. Reifsnider, "A time and hydration dependent viscoplastic model for polyelectrolyte membranes in fuel cells," *Mechanics of Time-Dependent Materials*, vol. 12, no. 1, pp. 15–30, 2008.

[28] Y. Tang, M. H. Santare, A. M. Karlsson, S. Cleghorn, and W. B. Johnson, "Stresses in proton exchange membranes due to hygro-thermal loading," *Journal of Fuel Cell Science and Technology*, vol. 3, no. 2, pp. 119–124, 2006.

[29] L. Yan, T. Gray, K. Patankar, S. Case, M. Ellis, R. Moore, D. Dillard, Y.-H. Lai, Y. Li, and C. Gittleman, "The nonlinear viscoelastic properties of pfsa membranes in water-immersed and humid air conditions," in *Experimental Mechanics on Emerging Energy Systems and Materials, Volume 5*, ser. Conference Proceedings of the Society for Experimental Mechanics Series. Springer New York, 2011, pp. 163–174.

[30] T. H. Yu, W.-G. Liu, Y. Sha, B. V. Merinov, P. Shirvanian, and W. A. G. III, "The effect of different environments on nafion degradation: Quantum mechanics study," *Journal of Membrane Science*, vol. 437, no. 0, pp. 276 – 285, 2013.

[31] K. D. Baik, B. K. Hong, and M. S. Kim, "Effects of operating parameters on hydrogen crossover rate through nafion membranes in polymer electrolyte membrane fuel cells," *Renewable Energy*, vol. 57, no. 0, pp. 234 – 239, 2013.

[32] D. Liu and S. Case, "Durability study of proton exchange membrane fuel cells under dynamic testing conditions with cyclic current profile," *Journal of Power Sources*, vol. 162, no. 1, pp. 521 – 531, 2006.

[33] G. Mousa, F. Golnaraghi, J. DeVaal, and A. Young, "Detecting proton exchange membrane fuel cell hydrogen leak using electrochemical impedance spectroscopy method," *Journal of Power Sources*, vol. 246, no. 0, pp. 110 – 116, 2014.

[34] A. Shah, T. Ralph, and F. Walsh, "Modeling and simulation of the degradation of perfluorinated ion-exchange membranes in pem fuel cells," *Journal of The Electrochemical Society*, vol. 156, no. 4, pp. B465–B484, 2009.

[35] W. Bi and T. F. Fuller, "Modeling of PEM fuel cell pt/c catalyst degradation," *Journal of Power Sources*, vol. 178, no. 1, pp. 188 – 196, 2008.

[36] R. M. Darling and J. P. Meyers, "Kinetic model of platinum dissolution in pemfcs," *Journal of The Electrochemical Society*, vol. 150, no. 11, pp. A1523–A1527, 2003.

[37] S. Dhanushkodi, M. Tam, S. Kundu, M. Fowler, and M. Pritzker, "Carbon corrosion fingerprint development and de-convolution of performance loss according to degradation mechanism in {PEM} fuel cells," *Journal of Power Sources*, vol. 240, no. 0, pp. 114 – 121, 2013.

[38] N. Hodnik, M. Zorko, B. Jozinovic, M. Bele, G. Drazic, S. Hocevar, and M. Gaberscek, "Severe accelerated degradation of PEMFC platinum catalyst: A thin film il-sem study," *Electrochemistry Communications*, vol. 30, no. 0, pp. 75 – 78, 2013.

[39] S. S. Kocha, "Chapter 3 - electrochemical degradation: Electrocatalyst and support durability," in *Polymer Electrolyte Fuel Cell Degradation*, M. M. Mench, E. C. Kumbur, and T. N. Veziroglu, Eds. Academic Press, 2012, pp. 89 – 214.

[40] M. F. Mathias, R. Makharia, H. A. Gasteiger, J. J. Conley, T. J. Fuller, C. J. Gittleman, S. S. Kocha, D. P. Miller, C. K. Mittelsteadt, T. Xie *et al.*, "Two fuel cell cars in every garage?" *Interface-Electrochemical Society*, vol. 14, no. 3, pp. 24–36, 2005.

[41] P. Parthasarathy and A. V. Virkar, "Electrochemical ostwald ripening of pt and ag catalysts supported on carbon," *Journal of Power Sources*, vol. 234, no. 0, pp. 82 – 90, 2013.

[42] N. Wagner and M. Schulze, "Change of electrochemical impedance spectra during co poisoning of the pt and pt - ru anodes in a membrane fuel cell pefc," *Electrochimica Acta*, vol. 48, pp. 3899 – 3907, 2003.

[43] Z.-M. Zhou, Z.-G. Shao, X.-P. Qin, X.-G. Chen, Z.-D. Wei, and B.-L. Yi, "Durability study of pt–pd/c as pemfc cathode catalyst," *international journal of hydrogen energy*, vol. 35, no. 4, pp. 1719–1726, 2010.

[44] S. Yu, X. Li, J. Li, S. Liu, W. Lu, Z. Shao, and B. Yi, "Study on hydrophobicity degradation of gas diffusion layer in proton exchange membrane fuel cells," *Energy Conversion and Management*, vol. 76, no. 0, pp. 301 – 306, 2013.

[45] L. Ceballos, "Caracterisation des proprietes fluidiques des couches de diffusion des piles a combustible pemfc par une approche numerique de type reseaux de pores et par une analyse d'images issues de la tomographie x," 2011.

[46] G. Chen, H. Zhang, H. Ma, and H. Zhong, "Electrochemical durability of gas diffusion layer under simulated proton exchange membrane fuel cell conditions," *International Journal of Hydrogen Energy*, vol. 34, no. 19, pp. 8185 – 8192, 2009.

[47] A. El-kharouf and B. G. Pollet, "Chapter 4 - gas diffusion media and their degradation," in *Polymer Electrolyte Fuel Cell Degradation*, M. M. Mench, E. C. Kumbur, and T. N. Veziroglu, Eds. Academic Press, 2012, pp. 215 – 247.

[48] J. Pauchet, M. Prat, P. Schott, and S. P. Kuttanikkad, "Performance loss of proton exchange membrane fuel cell due to hydrophobicity loss in gas diffusion layer: Analysis by multiscale approach combining pore network and performance modelling," *International Journal of Hydrogen Energy*, vol. 37, no. 2, pp. 1628 – 1641, 2012.

[49] A. Oyarce, N. Holmstrom, A. Boden, C. Lagergren, and G. Lindbergh, "Operating conditions affecting the contact resistance of bi-polar plates in proton exchange membrane fuel cells," *Journal of Power Sources*, vol. 231, no. 0, pp. 246 – 255, 2013.

[50] H. Tawfik, Y. Hung, and D. Mahajan, "Chapter 5 - bipolar plate durability and challenges," in *Polymer Electrolyte Fuel Cell Degradation*, M. M. Mench, E. C. Kumbur, and T. N. Veziroglu, Eds. Academic Press, 2012, pp. 249 – 291.

[51] F. Hizir, S. Ural, E. Kumbur, and M. Mench, "Characterization of interfacial morphology in polymer electrolyte fuel cells: Micro-porous layer and catalyst layer surfaces," *Journal of Power Sources*, vol. 195, no. 11, pp. 3463 – 3471, 2010.

[52] H. Bajpai, M. Khandelwal, E. Kumbur, and M. Mench, "A computational model for assessing impact of interfacial morphology on polymer electrolyte fuel cell performance," *Journal of Power Sources*, vol. 195, no. 13, pp. 4196 – 4205, 2010.

[53] T. Swamy, E. Kumbur, and M. Mench, "Characterization of interfacial structure in pefcs: water storage and contact resistance model," *Journal of The Electrochemical Society*, vol. 157, no. 1, pp. B77–B85, 2010.

[54] A. Franco, "Modelling and analysis of degradation phenomena in pemfc." Woodhead, 2012.

[55] L. Lu, M. Ouyang, H. Huang, P. Pei, and F. Yang, "A semi-empirical voltage degradation model for a low-pressure proton exchange membrane fuel cell stack under bus city driving cycles," *Journal of Power Sources*, vol. 164, no. 1, pp. 306 – 314, 2007.

[56] Z. Xinfeng, S. Yong, Z. Tong, and W. Zhen, "Statistic analysis on voltage degradation of pemfc under road environment," in *Proceedings of the International Conference on Future Electrical Power and Energy System*, 2012.

[57] U. D. of Energy. (2011) The department of energy hydrogen and fuel cells program plan. [Online]. Available: http://www.hydrogen.energy.gov/roadmaps_vision.html

[58] D. Hissel, M.-C. Péra, D. Candusso, F. Harel, and S. Bégot, "Characterization of polymer electrolyte fuel cell for embedded generators. test bench design and methodology," in *Advances in fuel cells*, X.-W. Zhang, Ed. Research Signpost, 2005.

[59] Y. Hou, Z. Yang, and G. Wan, "An improved dynamic voltage model of PEM fuel cell stack," *International Journal of Hydrogen Energy*, vol. 35, no. 20, pp. 11 154 – 11 160, 2010.

[60] X. Zhang, Y. Rui, Z. Tong, X. Sichuan, S. Yong, and N. Huaisheng, "The characteristics of voltage degradation of a proton exchange membrane fuel cell under a road operating environment," *International Journal of Hydrogen Energy*, no. 0, pp. –, 2014.

[61] A. Doucet, N. de Freitas, N. Gordon, and A. Smith, *Sequential Monte Carlo Methods in Practice*, ser. Information Science and Statistics. Springer, 2010.

[62] M. S. Arulampalam, S. Maskell, N. Gordon, and T. Clapp, "A tutorial on particle filters for online nonlinear/non-gaussian bayesian tracking," *Signal Processing, IEEE Transactions on*, vol. 50, no. 2, pp. 174–188, 2002.

[63] D. An, J.-H. Choi, and N. H. Kim, "A tutorial for model-based prognostics algorithms based on matlab code," in *Proceedings of the annual conference of the prognostics and health management society*, 2012.

Prof. Marie-Cécile Péra was born in 1968 in Paris, France. She received a PhD in electrical engineering from the Institut National Polytechnique de Grenoble, in 1993. From 1994 to 1999, she was associate professor at the University of Reims Champagne Ardennes, where she studied non-linear dynamics of electrical systems, based on chaos theory. Since 1999, she has joined the University of Franche Comté (UFC). In September 2008, she became a full Professor. She's the deputy director of the FEMTO-ST Institute. She's a researcher of the Energy Department of FEMTO-ST and a member of the FCLAB Research Federation. She develops models based on the Energetic Macroscopic Representation (EMR) of power generation system (fuel cells, PEMFC and SOFC, supercapacities, batteries), their control and the energy management. She works on diagnosis and prognosis of fuel cells. She has contributed to more than 200 publications in international scientific journals and international conferences.

Marine Jouin received her engineering degree from the National Engineering Institute in Mechanics and Microtechnologies of Besançon (ENSMM) in 2013. She joins AS2M and ENERGY departments of FEMTO-ST Institute the same year to start her Ph.D. She works on developing prognostics for proton exchange membrane fuel cells stacks based on hybrid approaches. She is also part of the FCLAB (Fuel Cell Lab) Research Federation (CNRS), devoted to Fuel Cell Systems Research and Technology.

Rafael Gouriveau received his engineering degree from National Engineering School of Tarbes (ENIT) in 1999. He then got his MS (2000), and his Ph.D. in Industrial Systems in 2003, both from the Toulouse National Polytechnic Institute (INPT). In September 2005, he joined the National Engineering Institute in Mechanics and Microtechnologies of Besançon (ENSMM) as Associate Professor. As for investigation, he is with the AS2M department of FEMTO-ST Institute. His research interests are in the development of industrial prognostics systems and the investigation of reliability modeling using possibility theory. He is also the scientific coordinator of PHM research axes from the FCLAB Research Federation (CNRS).

Prof. Noureddine Zerhouni received his engineering degree from National Engineers and Technicians School of Algiers (ENITA) in 1985. He received his Ph.D. Degree in Automatic Control from the Grenoble National Polytechnic Institute in 1991. In September 1991, he joined the National Engineering School of Belfort (ENIB) as Associate Professor. Since September 1999, Noureddine Zerhouni has been a Professor at the national high school of mechanics and microtechniques of Besançon. As for investigation, he is with AS2M department of FEMTO-ST Institute. His main research activities are concerned with intelligent maintenance systems, and PHM.

Prof. Daniel Hissel (M'03, SM'04) obtained an electrical engineering degree from the Ecole Nationale Supérieure d'Ingénieurs Electriciens de Grenoble in 1994. Then, he obtained a PhD from the Institut National Polytechnique de Toulouse in 1998. From 1999 to 2000, he worked for ALSTOM Transport in Tarbes (France) where he was system engineer on electrical and fuel cell buses projects. From 2000 to 2006, he has been an Associate Professor at the University of Technology Belfort. From 2006 to 2008, he has been a Full Professor at the University of Franche-Comté and Head of the "Fuel Cell Systems" Research Team of the Laboratory of Electrical Engineering and Systems. In 2008, he joined the FEMTO-ST (CNRS) Institute and became Head of the "Energy systems modelling" research team. Since 2012, he is the Head of the "Hybrid & Fuel Cell Systems" research team in the same Institute and also currently the Director of the FCLAB (Fuel Cell Lab) Research Federation (CNRS), devoted to Fuel Cell Systems Research and Technology. His main research activities are concerning fuel cell systems dedicated to automotive and stationary applications, modelling, non linear control and energy optimization of these systems and fuel cell system diagnosis. He was Associate Editor of IEEE Transactions on Industrial Electronics between 2004 and 2012 and is Associate Editor of ASME Fuel Cell Science and Technology. He is also the Chair of the IEEE VTS French Chapter and member of the advisory board of the MEGEVH network, the French national network on EV and HEV. He has published more than 290 scientific papers in peer-reviewed international journals and/or international conferences.